Localized charge injection in SiO_2 films containing silicon nanocrystals

Elizabeth A. Boer,[a] Mark L. Brongersma, and Harry A. Atwater
Thomas J. Watson Laboratory of Applied Physics, California Institute of Technology, Pasadena, California 91125

Richard C. Flagan
Department of Chemical Engineering, California Institute of Technology, Pasadena, California 91125

L. D. Bell
Jet Propulsion Laboratory, California Institute of Technology, Pasadena, California 91125

(Received 14 July 2000; accepted for publication 14 May 2001)

An atomic-force microscope (AFM) is used to locally inject, detect, and quantify the amount and location of charge in SiO_2 films containing Si nanocrystals (size $\sim$2–6 nm). By comparison with control samples, charge trapping is shown to be due to nanocrystals and not ion-implantation-induced defects in samples containing ion-beam-synthesized Si nanocrystals. Using an electrostatic model and AFM images of charge we have estimated the amount of charge injected in a typical experiment to be a few hundred electrons and the discharge rate to be $\sim 35 \pm 15$ e/min. © *2001 American Institute of Physics.* [DOI: 10.1063/1.1383574]

Future developments in nanoscale silicon electronics require tools for local manipulation and probing of stored charge. Charge storage and manipulation at the nanoscale is particularly important to nonvolatile floating gate memory devices such as nanocrystal-based memories[1] in which the floating gate consists of a dense array of Si nanocrystals embedded in the gate oxide. Such devices potentially offer both superior nonvolatile memory performance relative to conventional flash memories, and a simple design that is scalable to nanometer dimensions.[2] Silicon, with its mature technology, is the material of choice for these devices as structures can be fabricated cheaply and reliably. In general, however, nanoparticle synthesis methods introduce defects in the oxide host which can affect charge injection and retention.[3]

Traditional device analysis techniques such as capacitance–voltage measurements[3] give important macroscopic device information, but in order to probe the *local* properties of a device, a technique capable of detecting the presence and motion of a few localized charges is necessary. Conducting-tip atomic-force microscopy (AFM) is sensitive to a variety of forces, including electrostatic, thus making it a good tool for mapping weak electrostatic potentials[4,5] and capacitance[6] on the nanometer scale. It can also be used to inject electrons or holes into a localized region in materials such as polymers,[7] thin insulating films,[8] double-barrier $CeO_2/Si/CeO_2/Si$ structures,[9] and Co nanoclusters embedded in SiO_2.[10] For these reasons, an AFM is a useful tool to study the injection and dissipation of charge in SiO_2 films containing ion-beam-synthesized Si nanocrystals.[11] In this letter, we report on charge injection in silicon nanocrystal floating gates and show that charge trapping is due to the presence of nanocrystals and not defects from the implantation process. We develop and use a generalized force model of the tip–sample interaction and combine electrostatic modeling and AFM imaging to investigate the discharging dynamics of injected charge.

The samples investigated consist of a 100 nm wet thermally grown silicon-dioxide layer on light B-doped Si substrates that was implanted at room temperature with 35 keV Si^+ ions to a fluence of 4×10^{16} Si/cm^2. The samples were annealed at 1100 °C for 10 min in vacuum (base pressure $<8\times10^{-7}$ Torr) to allow the nucleation and growth of silicon nanocrystals (size $\sim$2–6 nm, as determined from transmission electron microscopy). Control samples consisted of (a) unimplanted and (b) Ar-implanted SiO_2 films, implanted at room temperature with 50 keV Ar^+ ions to a fluence of 2.9×10^{16} Ar/cm^2. The inert element argon and the particular ion energy and fluence were chosen so as to produce samples without nanocrystals, but with the same ion-implantation-damage profile as the Si-implanted samples [as calculated using TRIM (Ref. 12)]. The control samples were annealed as above. All samples were etched with buffered hydrofluoric acid[13] approximately halfway through the film, as measured by Rutherford backscattering spectroscopy, to eliminate contamination or surface defects from the vacuum anneal.[14]

The atomic-force microscope and highly doped Si tips were from commercial sources.[15] All images were taken in noncontact mode, with the sample stage grounded, in a box purged with N_2 gas (resulting humidity $<$10%). Charge was transferred from the AFM tip to the samples by applying a potential to the tip (typically, -10 V), disengaging the feedback of the microscope, then lowering the tip toward the sample surface. The distance between the tip and sample was monitored by observing the damping of the tip oscillations on an oscilloscope.[16] After contact and charge transfer, the feedback was reengaged, the AFM tip grounded, and images made (Fig. 1). Conventional AFM imaging was used to detect the injected charge.

Figure 1(a) and 1(c) show AFM images of etched Si nanocrystal and control samples. The morphology of the nanocrystal sample is different from that of the flat control sample, confirming the presence of nanocrystals. The particle

[a]Electronic mail: Elizabeth.Boer@alcatel.fr

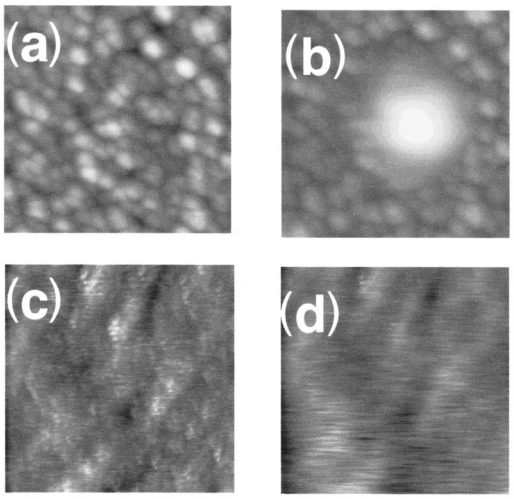

FIG. 1. Atomic-force microscope image of (a) an etched silicon-dioxide film containing silicon nanocrystals made by Si ion implantation and annealing before charging and (b) the same sample after charge transfer. Note that the injected charge is imaged as a protrusion on the surface. The lateral dimension for (a) and (b) is 0.5 μm. The vertical scale (black to white) is 15 nm for (a) and 25 nm for (b). (c) and (d) represent AFM images before and after charging of an etched silicon-dioxide film implanted with Ar^+ ions and annealed. Note that in this sample no localized charging is seen, indicating that charge is not trapped in defects from the implantation process. The lateral dimension for (c) and (d) is 1 μm. The vertical scale (black to white) for both is 1.5 nm.

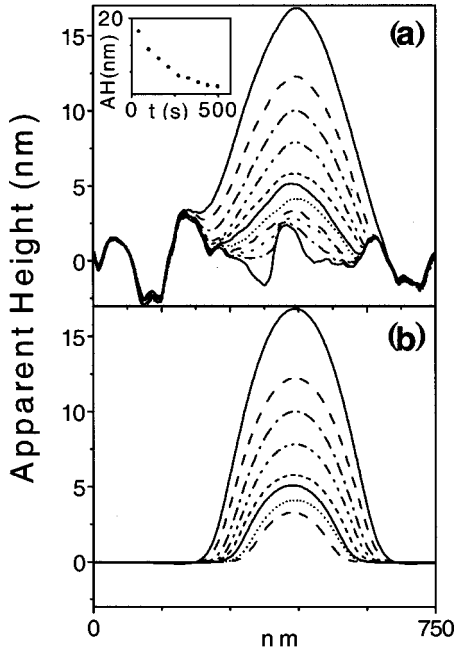

FIG. 2. (a) Cross-section time series of AFM images of trapped charge in a SiO_2 film containing silicon nanocrystals and (b) the corresponding fits to the data. The first trace is recorded 40±3 after charge injection, and each subsequent trace is recorded at 57 s intervals. The inset shows how the "apparent height" (or AH), from the maximum of the traces in (a), decreases with time. From the fits in (b), the amount and location of the trapped charge seen in each trace is determined and plotted in Fig. 3.

density is seen to be $\sim 6\times 10^{10}$ cm^{-2}, similar to that measured from transmission electron micrographs. The features are 1–4 nm high. Figure 1(b) shows localized charging in the nanocrystal samples, while the Ar-implanted control sample annealed at 1100 °C does not show this type of behavior [Fig. 1(d)]. This result indicates that nanocrystals are necessary for localized charging. The AFM image of charge appears as a protrusion on the surface due to the electrostatic interaction between the image charge in the grounded tip and the charge in the sample.

Figure 2(a) shows a discharging time series—vertical cross sections of subsequent AFM images are plotted on the same axes. In the inset to Fig. 2(a), the "apparent height" of the injected charge decreases from ~17 to 3 nm in 500 s. Figure 2(b) consists of the corresponding fits to the data, obtained by an iterative method explained below. In Fig. 3, the amount and spatial extent of the charge as a function of time is plotted, demonstrating that the spatial extent of the injected charge decreases with time. These results were determined using an electrostatic model as follows. The AFM tip was approximated by a grounded metallic sphere, and the electrostatic force interaction between the injected charge on the sample and the image charge in the grounded tip was calculated. The charge was assumed to be only on the sample surface, to reduce the complexity of the computation, but in principle the model could be easily expanded to include three-dimensional charge distributions. The charge distribution consisted of a disk upon which was imposed a grid (typical grid spacing, 5 nm). In principle, any arbitrary two-dimensional charge distribution may be assigned to this grid, but for a first approximation, the total assigned charge was uniformly distributed over the grid points. Polarization effects were ignored, as were effects on the tip motion due to the surrounding medium (such as hydrodynamic damping),[17] and the nanocrystal topography was replaced with a flat plane. The electrostatic interaction between the tip and sample was then found by taking each charged grid point, and finding the resultant image charge induced in the grounded tip. The total Coulomb force was subsequently calculated by summing up the interaction of each grid-point charge with each image charge, i.e.,

$$\vec{F}(\text{electrostatic}) = \sum_{i,j} \vec{F}_{ij} = \sum_{i,j} \frac{q_{s_i} q_{t_j}}{4\pi\varepsilon_0 D_{ij}^2} \hat{d}_{ij}, \qquad (1)$$

with q_{s_i} the ith grid-point charge on the sample, q_{t_j} the jth image charge in the tip, and D_{ij} the distance between them (and $\hat{d}_{ij}$ a unit vector). Thus, the total force was made up of two terms: one term due to the van der Waal interaction (between a sphere and plane),[18] and the second from the electrostatic contribution [Eq. (1)]. Only the z component of

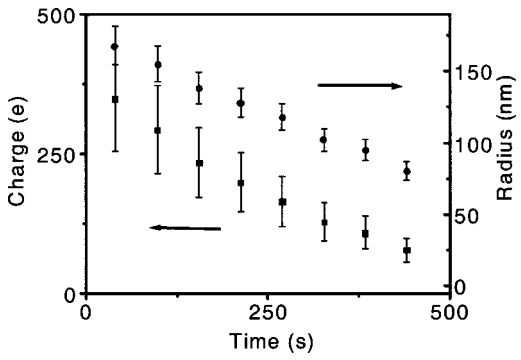

FIG. 3. Quantity and location of the injected charge as a function of time, as determined from the fits [in Fig. 2(b)] to the AFM discharging time series data [Fig. 2(a)]. Note the result that the area over which the charge is located decreases as the charge dissipates.

the total force was included since only the vertical forces on the tip were measured. It was assumed that the microscope feedback loop maintained the tip at a constant force gradient, set by and estimated from the imaging parameters, an assumption valid for small tip oscillation amplitudes (as compared to the tip–sample separation distance). This assumption holds when $F_{\text{Coulomb}} \gg F_{\text{van der Waals}}$, i.e., in the charged region. The equation

$$\left(\frac{\partial F_z}{\partial z}\right)_{\text{tot}} = \left(\frac{\partial F_z}{\partial z}\right)_{\text{vdW}} + \sum_{i,j}\left(\frac{\partial F_z}{\partial z}\right)_{ij} = \text{const}, \tag{2}$$

was solved (using Newton's method) for the height of the tip above the flat plane as it scanned over the charged region. This calculated profile was then compared to the data. By adjusting the initially assumed charge and charged area iteratively, a ''best fit'' was found.

From this analysis, it was determined that in a typical experiment $\sim 350 \pm 90$ electrons (of ~ 4 electrons per particle) are injected and leak away at a rate of $\sim 35 \pm 15e/\text{min}$. The decrease of the spatial extent of the charge with time suggests the main dissipation path is to the substrate (at a rate of ~ 0.2 nA/cm^2). Vertical transport may be via nanoparticles or via defects (from ion implantation or charge injection). Clear lateral dissipation was only seen in experiments done in air (i.e., humid environment).

In summary, we have shown that AFM is a useful technique to inject and detect charge on the nanoscale in technologically relevant materials such as Si nanoparticle-containing SiO_2 films. Using an atomic-force microscope, we have shown that the charge trap centers in annealed, Si-implanted silicon-dioxide films are due to the presence of nanocrystals and not simply due to process-induced defects in SiO_2. We have done calculations and have determined the magnitude of the injected charge and the rate of its dissipation.

The research described in this letter was jointly sponsored by the National Aeronautics and Space Administration (NASA) and the Jet Propulsion Laboratory Director's Research and Development Fund, and by the National Science Foundation under Grant No. DMR 98-71850.

[1] S. Tiwari, F. Rana, H. Hanafi, A. Hartstein, E. F. Crabbé, and K. Chan, Appl. Phys. Lett. **68**, 1377 (1996).
[2] L. Guo, E. Leobandung, and S. Y. Chou, Science **275**, 649 (1997).
[3] Y. Shi, K. Saito, H. Ishikuro, and T. Hiramoto, J. Appl. Phys. **84**, 2358 (1998).
[4] Y. Martin, D. W. Abraham, and H. K. Wickramasinghe, Appl. Phys. Lett. **52**, 1103 (1988).
[5] C. Schonenberger and S. F. Alvarado, Phys. Rev. Lett. **65**, 3162 (1990).
[6] C. C. Williams, J. Slinkman, W. P. Hough, and H. K. Wickramasinghe, Appl. Phys. Lett. **55**, 1662 (1989).
[7] B. D. Terris, J. E. Stern, D. Rugar, and H. J. Mamin, Phys. Rev. Lett. **63**, 2669 (1989).
[8] S. Morita, Y. Fukano, T. Uchihashi, T. Okusako, Y. Sugwara, Y. Yamanishi, and T. Oasa, Jpn. J. Appl. Phys., Part 2 **32**, L1701 (1993).
[9] J. T. Jones, P. M. Bridger, O. J. Marsh, and T. C. McGill, Appl. Phys. Lett. **75**, 1326 (1999).
[10] D. M. Schaadt, E. T. Yu, S. Sankar, and A. E. Berkowitz, Appl. Phys. Lett. **74**, 472 (1999).
[11] K. S. Min, K. V. Shcheglov, C. M. Yang, H. A. Atwater, M. L. Brongersma, and A. Polman, Appl. Phys. Lett. **69**, 2033 (1996).
[12] J. F. Ziegler, J. P. Biersack, and U. Littmark, *The Stopping and Range of Ions in Solids* (Pergamon, New York, 1985).
[13] From Transene Co. Inc.: 7.2% hydrofluoric acid, 36% ammonium fluoride, balance distilled water.
[14] Y. Takakuwa, M. Nihei, T. Horie, and N. Miyamoto, J. Non-Cryst. Solids **179**, 345 (1994).
[15] Thermomicroscopes (formally Park Scientific), 1171 Borregas Avenue, Sunnyvale, CA 94089.
[16] A. Bugacov, R. Resch, C. Baur, N. Montoya, K. Woronowicz, A. Papson, B. E. Koel, A. Requicha, and P. Will, Probe Microsc. **1**, 345 (1999).
[17] G. Y. Chen, R. J. Warmack, A. Huang, and T. Thundat, J. Appl. Phys. **78**, 1465 (1995).
[18] H. C. Hamaker, Physica (Amsterdam) **4**, 1058 (1937).